Flow, Turbulence and Combustion
https://doi.org/10.1007/s10494-023-00462-x

RESEARCH

Drag Assessment for Boundary Layer Control Schemes with Mass Injection

Georg Fahland[1] · Marco Atzori[2] · Annika Frede[1] · Alexander Stroh[1] · Bettina Frohnapfel[1] · Davide Gatti[1]

Received: 15 March 2023 / Accepted: 20 July 2023

Abstract
The present study considers uniform blowing in turbulent boundary layers as active flow control scheme for drag reduction on airfoils. The focus lies on the important question of how to quantify the drag reduction potential of this control scheme correctly. It is demonstrated that mass injection causes the *body drag* (the drag resulting from the stresses on the body) to differ from the *wake survey drag* (the momentum deficit in the wake of an airfoil), which is classically used in experiments as a surrogate for the former. This difference is related to the *boundary layer control (BLC) penalty*, an unavoidable drag portion which reflects the effort of a mass-injecting boundary layer control scheme. This is independent of how the control is implemented. With an integral momentum budget, we show that for the present control scheme, the wake survey drag contains the BLC penalty and is thus a measure for the *inclusive drag* of the airfoil, i.e. the one required to determine net drag reduction. The concept of the inclusive drag is extended also to boundary layers using the von Kàrmàn equation. This means that with mass injection the friction drag only is not sufficient to assess drag reduction also in canonical flows. Large Eddy Simulations and Reynolds-averaged Navier–Stokes simulations of the flow around airfoils are utilized to demonstrate the significance of this distinction for the scheme of uniform blowing. When the inclusive drag is properly accounted for, control scenarios previously considered to yield drag reduction actually show drag increase.

Keywords Uniform blowing · Turbulent boundary layer · Flow control

✉ Georg Fahland
georg.fahland@kit.edu

[1] Institute of Fluid Mechanics (ISTM), Karlsruhe Institute of Technology (KIT), Kaiserstr. 12, 76131 Karlsruhe, Baden-Württemberg, Germany

[2] Department of Aerospace Science and Technologies (DAER), Politecnico di Milano, Via La Masa 34, 20156 Milan, Italy

Published online: 15 August 2023

1 Introduction

Active flow control has been an ongoing area of research for many decades with the goal of improving the energy usage and performance of energy-intensive transport applications, such as civil aviation. The first active flow control was introduced by Prandtl who proposed to use suction in order to prevent separation in the adverse pressure gradient region of boundary layers [Schlichting and Gersten 2000, p.42]. In addition, boundary layer suction can also have the beneficial effect of delaying the transition from a laminar to a turbulent boundary layer (TBL) (Gregory et al. 1953). Transition delay allows to reduce the power requirements of internal or external flows, since the skin friction drag exerted by a laminar boundary layer is substantially lower than the one of a turbulent boundary layer. For aeronautic applications this is still a very active research field with sizeable potential for reducing the fuel consumption (Beck et al. 2018; Schrauf and von Geyr 2020). Recently, commercial aircraft industry adapted first implementations on the Boing 787 tailplane (Krishnan et al. 2017).

Despite the efforts to control turbulent transition, a turbulent boundary layer will eventually emerge along most applications. Substantial research has been devoted to the question of how to reduce viscous drag in turbulent boundary layers (Wilkinson et al. 1988; Spalart and McLean 2011), since this is one of the key contributions to the total drag of an airfoil (Bushnell 2003). Riblets, a particularly designed surface corrugation, are a successful example of a drag reducing passive (i.e. not requiring additional energy input) control technique. Thanks to their simplicity and passive nature, riblets have been already tested and proved working on aircraft (Walsh 1986). However, the maximum local skin-friction drag reduction achievable via passive strategies is typically limited to few percent and achievable only in specific operating conditions. Active drag-reducing flow control aims to overcome these limitations, albeit at the cost of an additional energy input. Among the simplest active control strategies for skin-friction drag reduction, blowing a small mass flow into the TBL has been proposed. In contrast to lift control via wall-parallel blowing in the aft region of an airfoil (von Glahn 1958; Norton 2002; Rumsey and Nishino 2011), drag-reducing blowing, sometimes referred to as micro blowing, is oriented in the wall-normal direction. First implementation efforts for wall-normal uniform blowing technique date back to the 1960 s (Kinney 1967; Moffat and Kays 1968; Simpson et al. 1969), after that the scheme regained interest based on direct numerical simulation (DNS) studies in the 1990 s (Sumitani and Kasagi 1995; Park and Choi 1999). A comprehensive review in Hwang (2004) includes experimental and numerical efforts towards practical implementation. In this review the achieved skin friction reduction with micro blowing is reported to reach 50% in subsonic flow and more than 80% for supersonic flow conditions.

A number of numerical studies concentrate on the properties of a flat plate TBL with uniform wall-normal blowing (Kametani and Fukagata 2011; Kametani et al. 2016; Stroh et al. 2016; Atzori et al. 2020). In the region of blowing a reduction of the skin-friction drag is found which is also maintained downstream of the controlled region. This constitutes a major difference compared to most other drag reducing techniques including laminar flow control. The difference is caused by the fact that uniform blowing increases the momentum deficit boundary layer thickness due to the added mass (that needs to be accelerated) while other skin-friction reducing control techniques (including transition control) lead to a smaller boundary layer growth rate due to the reduced viscous momentum loss (Stroh et al. 2016). A thinner boundary layer downstream of a

controlled section indicates a local drag increase compared to the uncontrolled flow. In consequence, the global benefit of e.g. laminar flow control is smaller than the local one (Spalart and McLean 2011).

The question of whether uniform blowing can be employed to reduce the global total drag of a finite size body has been repeatedly addressed in literature (Mickley 1954; Park and Choi 1999; Hwang 2004). Generally, the displacement effect of the boundary layer which induces a skin friction drag reduction even downstream of the controlled region is expected to increase the (viscous) contribution of pressure drag on the airfoil thus mitigating or cancelling the global total drag reduction (Spalart and McLean 2011).

In apparent contradiction to this expectation numerical studies of airfoils with blowing reveal a significant reduction of the total drag experienced by the airfoil (Atzori et al. 2020; Ohashi et al. 2020). Furthermore, it was shown that the scheme of uniform blowing on the pressure side of an airfoil has a prospect of significant performance enhancement resulting from both pressure and friction drag reduction (Fahland et al. 2021). In these studies, the total drag of the body is obtained through an integration of all shear stress and pressure along its surface.

In experimental studies the total drag on the airfoil is usually not measured directly. This is mainly related to the large ratio between lift and drag force which induces large uncertainties in direct drag force measurements. Wind tunnel measurements of airfoil drag are thus often based on wake measurements. This is also the case for experiments with micro blowing which showed partially good agreement with numerical results but also revealed some considerable deviations (Eto et al. 2019; Hasanuzzaman et al. 2020; Kornilov and Boiko 2012; Kornilov 2021; Miura et al. 2022). Eto et al. (2019) report drag reduction based on numerical results which was difficult to reproduce experimentally. Hwang [p. 569, Hwang 2004] describes good agreement between numerical results and experimental skin-friction reduction data measured with a balance, but observed the contradicting result of a drop in total pressure in the wake survey, which corresponds to a drag increase.

This contradicting evidence between numerical and experimental studies, or equivalently between the drag force measured directly on the body and indirectly from the wake, can be partially traced back to the uncertainties of both approaches. From the experimental side, for instance, there are uncertainties related to the extraction of the total drag based on wake measurements and different corrections have been proposed for wind tunnel experiments to deal with the finite control volume size, resulting e.g. in the methods of Betz (1925) and Jones (1937). However, the major reason for the disagreement mentioned above can be linked to the contribution of micro blowing to the momentum balance. For instance, if the mass of the control fluid is assumed to be available from a source within the airfoil, the drag force deduced from the wake is larger than the body drag, as recently discussed by [Supplemental Material, Fahland et al. 2021]. This difference is a possible explanation for the fact that experiments on airfoils with micro blowing, where drag is retrieved from wake measurement, yield less-promising results than the corresponding numerical studies (Eto et al. 2019), where drag is typically more comfortably obtained by integration of the stresses along the body surface.

In the present work we analyze the relation between the total drag of an airfoil measured directly at its surface or in its wake based on well-resolved LES and RANS numerical data for incompressible and compressible flows. Aided by such numerical results, we address the question whether the force exerted from the flow onto the airfoil or the force deduced from the wake survey is relevant for the performance measurement of micro blowing for skin-friction drag reduction on airfoils.

Several authors approached this subject in the past, e.g. by considering the momentum budget (e.g. [Mickley (1954), p. 30]) or evaluating the energy requirement of the mass-injecting control for different scenarios (Fahland et al. 2021; Hirokawa et al. 2020). However, most studies within the field of turbulent skin friction drag reduction focus on the friction drag only leveraging canonical cases such as ducts or flat plates which do not yield other obvious drag components. Therefore, the question about additional cost is usually out of scope. Yet, we show that the momentum budget analysis gives a general answer about the theoretical penalty of this boundary layer control scheme prior to considering any implementation-dependent losses subject to optimization. This is done by carefully examining common assumptions in respect to the momentum budget of (turbulent) boundary layers with wall-normal blowing and their wakes.

2 Momentum Budget of Flow Around an Airfoil

We consider the integral momentum balance of a flow over a 2D airfoil with the control volume ABCD sketched in Fig. 1. As shown in the figure, the direction of the inflow and thus the direction of the drag force F_D coincides with $\overline{X}$. The corresponding normal direction and thus the direction of the lift force F_L is denoted by $\overline{Y}$. To allow for different angles of attack the orientation of the airfoil is described by a rotated coordinate system X, Y. Flow control due to wall-normal micro blowing on the pressure side of the airfoil is denoted by v_{BLC} and is assumed to be oriented in $\overline{Y}$-direction for small angles of attack. For the uncontrolled case $v_{\mathrm{BLC}} = 0$ applies. The control volume boundaries consist of the outer perimeter with the planes $\overline{AB}$ and $\overline{CD}$, aligned with the flow direction $\overline{X}$, and planes $\overline{BC}$ and $\overline{DA}$ which are parallel to $\overline{Y}$. At the wake survey plane $\overline{BC}$ we define a sampling coordinate s for pressure $p(s)$ and velocity $u(s)$. All other control volume boundaries are placed at a sufficiently large distance from the airfoil (e.g. 2/3c from the trailing edge [Russo 2011, ch. 7.2.3)] such that the velocity component in $\overline{X}$-direction $u_{\overline{X}}$ and pressure p along these boundaries can be assumed to

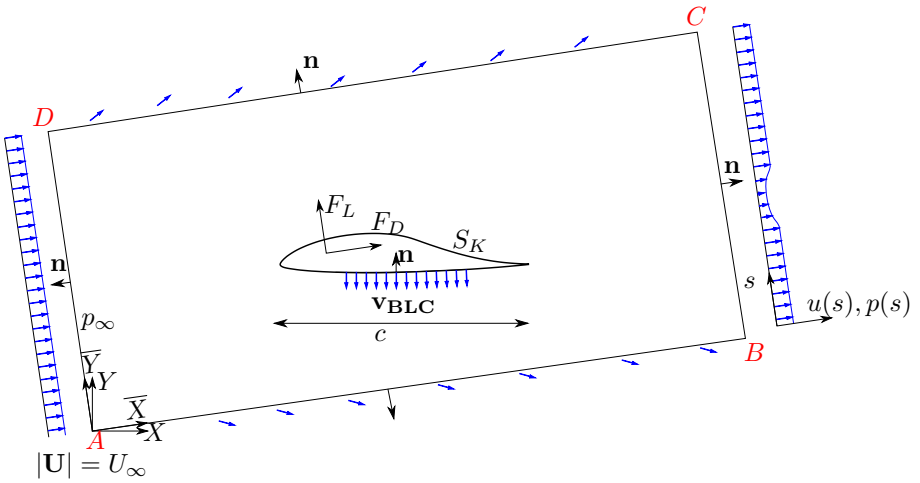

Fig. 1 Control Volume (CV) for the airfoil momentum budget in which **n** is the normal vector pointing out of the CV

correspond to the inflow conditions at infinite distance upstream of the airfoil. The wetted surface of the airfoil is denoted by S_K. Normal vectors $\mathbf{n}$ point out of the control volume.

The momentum budget for the flow in Fig. 1 without flow control ($v_{\mathrm{BLC}} = 0$) yields the well-known result that the force exerted from the fluid onto the airfoil in the mean flow direction ($\overline{X}$) can be recovered from the momentum deficit in the wake far downstream of the airfoil where the static pressure has recovered to its far upstream inflow value. The drag coefficient retrieved by integrating the stresses acting on the body (airfoil) is denoted with $c_{\mathrm{d,B}}$ and defined as

$$c_{\mathrm{d,B}} = \frac{2F_D}{\rho U_\infty^2 S_{\mathrm{ref}}}, \tag{1}$$

where S_{ref} is the product of chord length c and the span-wise airfoil dimension. Equivalently, the wake-survey also delivers the drag coefficient, which we denote with $c_{\mathrm{d,W}}$, as follows:

$$c_{\mathrm{d,W}} = \int_B^C \frac{2}{c}\frac{u(s)}{U_\infty}\left(1 - \frac{u(s)}{U_\infty}\right) ds. \tag{2}$$

We refer to $c_{\mathrm{d,W}}$ as *wake survey drag*. For an airfoil without blowing control, the *body drag* and *wake survey drag* are equivalent up to possible measurement uncertainties, i.e.

$$c_{\mathrm{d,B}} = c_{\mathrm{d,W}} \qquad \text{if } v_{\mathrm{BLC}} = 0. \tag{3}$$

The distinction between *body drag* $c_{\mathrm{d,B}}$ and *wake survey drag* $c_{\mathrm{d,W}}$ will become relevant for the controlled flow.

Under turbulent flow conditions, the velocity components in Eq. 2 correspond to temporally averaged values and an additional momentum flux due to the corresponding turbulent velocity fluctuations (and thus the Reynolds stresses in the time averaged scenario) is present such that

$$c_{\mathrm{d,W}} = \int_B^C \frac{2}{c}\frac{u(s)}{U_\infty}\left(1 - \frac{u(s)}{U_\infty}\right) ds + \int_B^C \underbrace{\frac{2}{c}\left(-\frac{\overline{u'^2}(s)}{U_\infty^2} + \frac{\overline{v'^2}(s)}{U_\infty^2}\right)}_{\text{Reynolds stress integrand } f_{\mathrm{ReStress}}} ds. \tag{4}$$

The additional momentum flux due to turbulent fluctuations were discussed for free shear layers [Townsend 1976, p. 93] but are rarely measured experimentally since their contribution to the drag coefficient is small even close to the airfoil trailing edge where high turbulence intensities are found [Schlichting 1964, p.703]. It will be shown that the turbulent contributions to $c_{\mathrm{d,W}}$ are also negligibly small for the present investigation.

If the static pressure along the wake survey plane $\overline{BC}$ has not recovered to its far upstream value, Eq. 2 has to be extended to

$$c_{\mathrm{d,W}} = \int_B^C \underbrace{\frac{2}{c}\frac{u(s)}{U_\infty}\left(1 - \frac{u(s)}{U_\infty}\right) + \frac{2}{c\rho U_\infty^2}\left(p_\infty - p(s)\right)}_{\text{wake survey integrand } f_{\mathrm{WS}}} ds. \tag{5}$$

Since the experimental determination of $u(s)$ or $p(s)$ can be challenging, alternative extensions to Eq. 2 are available in literature (Betz 1925; Jones 1937). For numerical data sets Eq. 5 can be applied directly. If any drag reducing flow control is realized on the airfoil without the addition or removal of mass inside the control volume, e.g. riblet-induced drag reduction, we expect a reduction of $c_{\mathrm{d,B}}$ that can be deduced from the wake survey following Eqs. 2 or 5 under the same assumptions as for the uncontrolled flow.

In the case of the active flow control scheme of micro blowing a source of mass is added into the airfoil which leaves the airfoil at speed v_{BLC} normal to the mean flow direction. Micro blowing on the pressure side of the airfoil is sketched in Fig. 1. Note that the injected control fluid does not carry any momentum in the streamwise direction (if we consider the flow in the airfoil reference system as indicated in Fig. 1). It is known that this particular type of micro blowing on the pressure side can reduce not only the skin friction drag but also the pressure drag along the airfoil (Atzori et al. 2020; Fahland et al. 2021). The force F_D that the surrounding fluid exerts onto the airfoil, and thus $c_{\mathrm{d,B}}$ (see Eq. 1), is reduced in this setting. However, due to the mass added inside the control volume, this change in force does not directly reflect in the wake flow. The fact that the injected mass flow for boundary layer control (BLC) has to be accelerated in streamwise direction causes an additional momentum deficit in the wake. This momentum deficit is given by the product of BLC mass flow rate and U_∞ which can be normalized in analogy to a drag coefficient (see Eq. 1) to obtain a dimensionsless number, c_{BLC}, that describes a BLC penalty. In the case of BLC control with (mass injecting) blowing the dimensionless momentum balance reads

$$c_{\mathrm{d,B}} + \underbrace{2\frac{v_{\mathrm{BLC}}}{U_\infty}\frac{l_{\mathrm{BLC}}}{c}}_{c_{\mathrm{BLC}}} = c_{\mathrm{d,W}}. \tag{6}$$

The BLC penalty thus describes the difference between *body drag* and *wake survey drag* in the blowing-controlled configuration. Large blowing rates can induce significant differences between the drag measured directly at the airfoil and the momentum deficit of the wake. Eq. 6 indicates that $c_{\mathrm{d,B}}$ may even assume negative values if $c_{\mathrm{BLC}} > c_{\mathrm{d,W}}$ which is later shown in Fig. 4. In the derivation of Eq. 6 the mass flow required for micro blowing flow control originates from an unknown source. It is simply assumed to be available on the controlled surface. In numerical simulations this is achieved through the definition of a suitable boundary condition. In experiments an external pressurized reservoir from which fluid is guided into the airfoil has to be made available.

More realistically, one may consider the collection of the required control fluid as a separate problem, where instead of a reservoir an air intake is utilised. The air intake redirects the collected fluid so that ultimately all its $\overline{X}$-momentum is transferred to the body. Even if viscous losses are neglected, this loss of $\overline{X}$-momentum causes an additional drag component at the intake which equals the term c_{BLC} albeit being of opposite sign. The difference of the wake-survey drag and the *body drag* of the airfoil-intake system still respects Eq. 6. In fact, the air-collection and the BLC only form a closed system in terms of mass continuity if considered simultaneously: in this case the equality of *body drag* and *wake survey drag* is restored. If the airfoil with BLC is considered without an air-intake, i.e. a mass source is present, the BLC penalty c_{BLC} has to be considered.

An ideal fluid collection happens without total pressure losses. In consequence the collected fluid is available at a static pressure equal to the total pressure of the freestream. We note that collection of control fluid at stagnation pressure conditions provides a “power reservoir" since the collected fluid has a higher pressure than the static pressure at the location

of the BLC. In this ideal case, there is at least some pressure difference available to overcome implementation-dependent losses (such as viscous losses of forcing the fluid through a porous surface) thus enabling a system of passive blowing as it has been described e.g. by Hirokawa et al. (2020). Theoretically, it may also be possible to harvest the pressure difference mentioned above, as explained e.g. by Fahland et al. (2021) who showed using energetic considerations that the BLC penalty drag coefficient c_{BLC} in this case would reduce to only half of what is obtained here from the momentum balance. This is because the increased pressure level upon fluid collection is not a necessary condition in terms of the energy budget but a result from the circumstance that a lossless collection of BLC fluid can only happen at total pressure and not below. However, any attempt of energy recovery by expanding fluid through a recovery system is limited by viscous losses within the system itself, in addition to losses within the propulsive system exploiting the regained power to counteract the total drag of the aircraft. Therefore, any attempt of even marginally reducing the momentum-budget-based BLC penalty c_{BLC} remains very inefficient and thus not viable due to inefficiencies in energy recovery as well as the additional mass of the recovery system. Therefore, the momentum-budget based BLC-penalty c_{BLC} derived here is a very reasonable measure of the unavoidable costs of the control scheme of uniform blowing.

Appendix A shows that carrying a reservoir of pressurised air for providing the BLC fluid is indeed not a viable alternative to fluid collection either: a cruise flight mission with a range of 4000 kms would require the sizeable additional mass of 280.000 kgs. In this scenario, an additional force is required to accelerate the mass of the control fluid to flight speed. The impulse of such force is equivalent to the time-integrated force of collecting the fluid in flight. The supply of control fluid from an external source or its carrying thus inevitably leads to additional force requirements that are not included in force measurements directly at the airfoil. As a result the *wake survey drag* yields a reasonable estimate of the total force required to move an airfoil with BLC at U_∞ not matter the source of the control fluid. While this result might be considered as obvious to some degree, we are not aware of recent literature references that clearly links *body drag* and *wake survey drag* in the form of Eq. 6 for the flow control scheme of uniform blowing.

In the following, we compare *body drag* and *wake survey drag* based on numerical simulations carried out for an airfoil with micro-blowing flow control. Both incompressible and compressible flow scenarios are considered. The relevant expressions obtained in this section can be easily extended to compressible flow conditions by accounting for the difference between ρ_∞, i.e. the density of the incoming flow at speed U_∞ and pressure p_∞, and the local density ρ. As a result, the drag coefficient $c_{\mathrm{d,W}}$ obtained via the wake survey, i.e. the compressible version of Eq. 5, reads

$$c_{\mathrm{d,W}} = \frac{2}{\rho_\infty c} \int_B^C \underbrace{\rho(s)\frac{u(s)}{U_\infty}\left(1-\frac{u(s)}{U_\infty}\right)+\frac{1}{U_\infty^2}\left(p_\infty - p(s)\right)}_{\text{wake survey integrand } f_{\mathrm{WS}}} ds. \tag{7}$$

Similarly, the relationship between the drag coefficient $c_{\mathrm{d,B}}$ measured on the body and $c_{\mathrm{d,W}}$ through the wake survey is as follows:

$$c_{\mathrm{d,B}} + \underbrace{2\frac{v_{\mathrm{BLC}}}{U_\infty}\frac{l_{\mathrm{BLC}}}{c}\frac{\rho_{\mathrm{BLC}}}{\rho_\infty}}_{c_{\mathrm{BLC}}} = c_{\mathrm{d,W}}. \tag{8}$$

3 Numerical Results

3.1 Drag Assessment for Flows Around Airfoils

The present analysis relies on Large Eddy Simulations (LES) and Reynolds-Averaged Navier–Stokes Simulations (RANS) data, where the latter are availalbe for incompressible and compressible flow conditions.

In the case of LES we consider the flow around a NACA4412 airfoil with and without uniform blowing. The setup of these simulations are extensively described by Vinuesa et al. (2018) for the uncontrolled reference case, while cases with control are described by Atzori et al. (2020). The portion of the data set that we examine in the present study consists of cases at a chord Reynolds number of $Re_c = U_\infty c/\nu = 400,000$, where U_∞ and ν are the velocity of the incoming flow and the kinematic viscosity of the fluid, respectively, and an angle of attack $\alpha = 5\circ$. These simulations are carried out using the code *Nek5000* Fischer et al. (2008), which is based on the spectral-element method proposed by Patera (1984). We employ a C-type mesh that extended up to a distance of $2c$ from the airfoil surface and $0.1c$ in the periodic direction. A precursor RANS simulation is used to impose inlet boundary conditions and the outflow boundary condition is implemented as proposed by Dong et al. (2014). The laminar-to-turbulent transition is enforced by the placement of tripping at $x/c = 0.1$, as proposed by Schlatter and Örlü (2012). The mesh is designed in the way that the grid spacing scaled in viscous units in the wall-normal, wall-tangential, and periodic directions are, respectively, $\Delta x_t^+ = 18$, $\Delta y_n^+ = (0.64, 11)$, and $\Delta z^+ = 9$ in the turbulent region of the domain resulting in approximately 463×10^6 grid points. The time step is selected to keep the CFL number of approximately 0.3. The adopted LES filter corresponds to the one proposed by Schlatter et al. (2004). A statistical convergence is ensured by the temporal integration for more than 10 flow-over times after the statistically stationary state has been reached. A validation with the DNS data of Hosseini et al. (2016) shows an excellent agreement for the uncontrolled case (Vinuesa et al. 2018).

The incompressible RANS of the flow around the same NACA4412 airfoil is carried out based on the setup of Fahland et al. (2021). This employs the simpleFoam solver from OpenFOAM simulation framework (Weller et al. 1998). Turbulence is modeled using the Menter k-ω-SST model (Menter et al 2003). While we considered multiple angles of attack ranging $\alpha = [-3\circ, 12\circ]$ and Reynolds number $Re_c = [0.1, 4] \cdot 10^6$, we limit the presented results to $\alpha = 5\circ$ and $Re_c = 4 \cdot 10^5$.

The compressible RANS simulations also consider the NACA4412 airfoil and are performed with the density-based steady-state solver from the open source CFD software SU2 (Economon et al. 2016). As for the incompressible case, the Menter k-ω-SST model is employed, whereas the grid generation system, size and resolution for a given Reynolds number are the same as in (Fahland et al. 2021), as well as the forced transition strategy, which imposes transition at $x/c = 0.1$. The fluid is modeled as standard air treated as an ideal gas with constant viscosity. The non-reflective far-field boundary condition is imposed at the outer boundaries of the computational domain based on the local direction of the characteristics. The airfoil surfaces are modeled as adiabatic walls. In the airfoil sections where wall transpiration is applied, wall velocity is imposed while the wall mass and energy fluxes are computed by extrapolating the thermodynamic properties via the Riemann invariants. The convective fluxes are discretised via the second-order Roe method, while the Green–Gauss method is employed for the viscous fluxes. A second-order upwind scheme is applied for gradients of turbulent

variables. A parametric study was performed where different parameters such as the Reynolds number, the Mach number, the angle of attack, the airfoil shape and the control velocity were investigated. For the sake of the present manuscript, we will present a subsonic case at a chord-based Reynolds number of $Re = 5 \cdot 10^6$, compatibly with the incompressible RANS case, a Mach number of $Ma = 0.4$ and an AoA of $\alpha = 0°$. For this case, the freestream flow and fluid parameters are $\rho = 1.169 \frac{\text{kg}}{\text{m}^3}$, $p = 100010\text{Pa}$ and $T = 298\text{K}$.

Wall-normal blowing is applied with intensity in the range $v_{\text{BLC}}/U_\infty = [0.1, 5]\%$ on either suction or pressure side of the airfoil. The blowing region on the suction side spans the interval $x/c = [0.25, 0.86]$, whilst it is placed at $x/c = [0.2, 1.0]$ on the pressure side alternatively.

The numerical data is evaluated in a control volume as indicated in Fig. 1 following Eq. 5. Data evaluation based on the methods suggested by Betz (1925) and Jones (1937), that rely on $u(s)$ only, was additionally carried out for the uncontrolled flow. The obtained RANS results for incompressible flow indicate that uncertainties in the *body drag* evaluation based on wake flow measurements (either following Eq. 5 or as suggested by Betz (1925) and Jones (1937)) are limited to less than 5% of the body drag for wake survey planes $\overline{BC}$ located at a down stream distance of $d_{\text{TE}}/c \approx [0.8, 2]$ behind the airfoil trailing edge. This is in reasonable agreement with literature suggestions, where an uncertainty of 2% is reported [2011, ch. 7.2.3].

We note that the commonly stated assumption of $u_{\overline{X}} = U_\infty$ and $p = p_\infty$ on all other control volume boundaries except the wake survey plane (see Sect. 2) is locally not valid for the present data set. This can easily be explained by the properties of a inviscid flow field around an airfoil: Although all values converge to the far-field values for increasing control volume size even small deviations add up when considering control volume faces such as $\overline{CD}$ in Fig. 1 separately. However, the integrated contribution of these local deviations from the idealized assumption over all control volume surfaces is small, such that the expected good agreement of the integral values is obtained nevertheless.

The computational box size of the LES data is too small to fulfill the requirement of $d_{\text{TE}}/c \geq 0.8$ behind the airfoil trailing edge. The *wake survey drag* is thus not expected to quantitatively agree with the body drag. Nevertheless, the distribution of the integrands labelled in Eqs. 4 and 5 reveal general properties of the applied control and can be considered to cross-check the (ir)relevance of the Reynolds stress contributions in the wake deficit. These values are plotted in Fig. 2 for blowing on the suction side (SS) and blowing on the pressure side (PS) at $d_{\text{TE}}/c = 0.2$, both in comparison to the uncontrolled reference case. The momentum deficit of the mean flow and the Reynolds stresses are plotted along s/c. As discussed above the turbulent contribution is small and the present data shows that the applied control induces only minor changes to this contribution. Comparing the mean flow contributions to the momentum deficit in the wake for the two different control scenarios (blue curves in Fig. 2) reveals significant differences. Blowing on the suction side deflects the wake upwards which is related to a substantial thickening of the boundary layer due to blowing in a region of adverse pressure gradient (Atzori et al. 2020) thereby reducing circulation/lift. The boundary layer on the pressure side of the airfoil is similar to a ZPG boundary layer resulting in a smaller growth of the boundary layer thickness due to the applied blowing compared to the suction side. Therefore, the corresponding downward deflection of the wake is less pronounced. Blowing on the suction side obviously results in a significant increase in the total wake deficit. The wake deficit is modified less for the case of blowing on the pressure side but still exhibits a total increase compared to the reference case despite the fact that the *body drag* of this case is reduced.

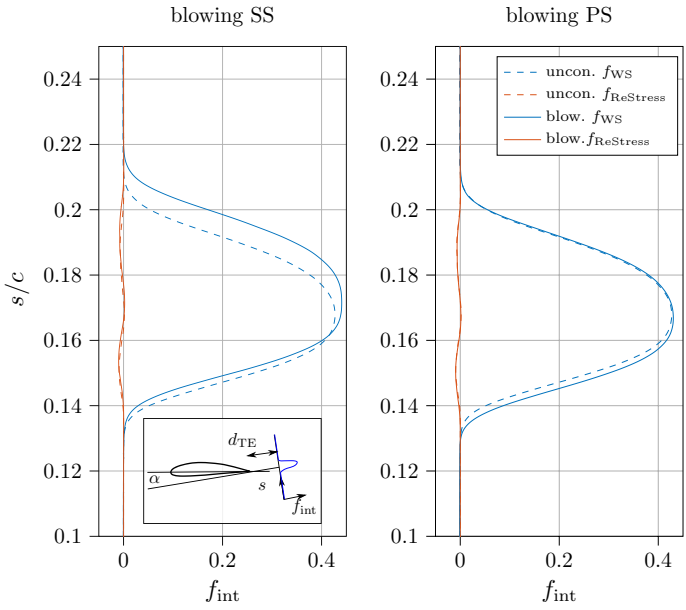

Fig. 2 LES-based wake profile f_{WS} (Eq. 5) and Re-Stresses $f_{ReStress}$ (Eq. 4) for blowing on the SS and blowing on the PS at $d_{TE}/c = 0.2$ behind the trailing edge. NACA 4412, angle of attack $\alpha = 5\circ$, $Re = 4 \cdot 10^5$, $v_{BLC} = 0.1\%U_\infty$

The fact that the *wake survey drag* is neither reduced for blowing on the pressure side nor on the suction side is also found for the RANS data for larger v_{BLC}. Figure 3 shows the *wake survey drag* $c_{d,W}$ in comparison to the sum of *body drag* and BLC penalty $c_{d,B} + c_{BLC}$ for one selected case. In agreement with literature results, it can be seen that blowing on the suction side increases the *body drag* (in green) while blowing on the pressure side decreases this value. However, the *wake survey drag* (in red) increases for both flow control scenarios. For both control cases, the sum of *body drag* and BLC penalty is in reasonable agreement with the *wake survey drag* as suggested by Eq. 5. Therefore, neither control technique is successful in the sense of a reduced force requirement

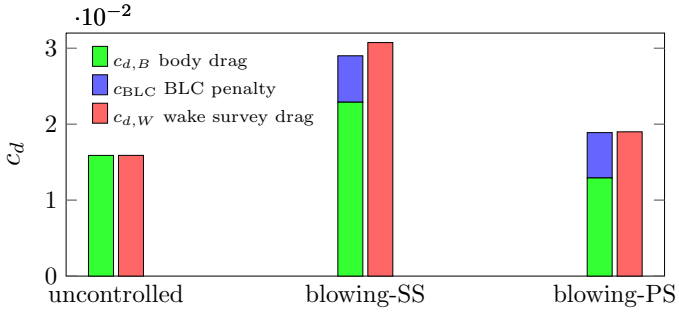

Fig. 3 Comparison of *wake survey* drag, *body drag* and *BLC penalty* based on incompressible RANS data. NACA 4412, $Re = 4 \cdot 10^5$, $v_{BLC} = 0.5\%U_\infty$, $d_{TE}/c = 0.8$, $h/c = 1.1$

for propulsion. In the case of PS blowing the gain of a reduced *body drag* is annihilated by the BLC penalty.

The effect of increased blowing intensity $v_{\mathrm{BLC}}/U_\infty$ on the global drag coefficients is shown in Fig. 4. The left part of the figure corresponds to blowing on the suction side of the airfoil for which the *body drag* increases in general. The contributions of friction and pressure drag to the *body drag* $c_{\mathrm{d,B}}$ are marked in color. It can be seen that the pressure drag strongly increases with increasing blowing intensity. The skin friction drag is reduced by blowing as expected and converges to a constant value for $v_{\mathrm{BLC}}/U_\infty > 1\%$ (for the present configuration) which stems from the friction contribution of the uncontrolled parts of the surface. Since blowing is applied in an adverse pressure gradient boundary layer, the controlled flow region becomes susceptible to separation and strong flow separation is observed for $v_{\mathrm{BLC}}/U_\infty > 0.5\%$. The boundary layer control penalty c_{BLC} increases linearly with $v_{\mathrm{BLC}}/U_\infty$ and needs to be considered on top of $c_{\mathrm{d,B}}$ as discussed above.

The case of blowing on the pressure side of the airfoil is shown in the right part of Fig. 4. Note that the vertical axis is scaled differently than in the left part of the figure. The friction drag contribution develops very similar to the case of blowing on the suction side. However, the pressure drag contribution exhibits a distinctly different behavior. As previously discussed by Fahland et al. (2021), it continuously decreases with increasing blowing intensity. For $v_{\mathrm{BLC}}/U_\infty > 2\%$ the pressure drag switches signs indicating a negative contribution to the *body drag* which leads to negative $c_{\mathrm{d,B}}$ for $v_{\mathrm{BLC}}/U_\infty > 3.2\%$. In this flow control regime, the airfoil itself thus experiences a negative drag, or in other words a thrust in upstream direction. This counter-intuitive phenomenon comes at a cost translated into c_{BLC}. The sum of $c_{\mathrm{d,B}}$ and c_{BLC} constantly increases with $v_{\mathrm{BLC}}/U_\infty$ indicating that the total force required to move the airfoil with BLC at U_∞ does never fall below the uncontrolled reference case. As discussed above this total force requirement is reflected in

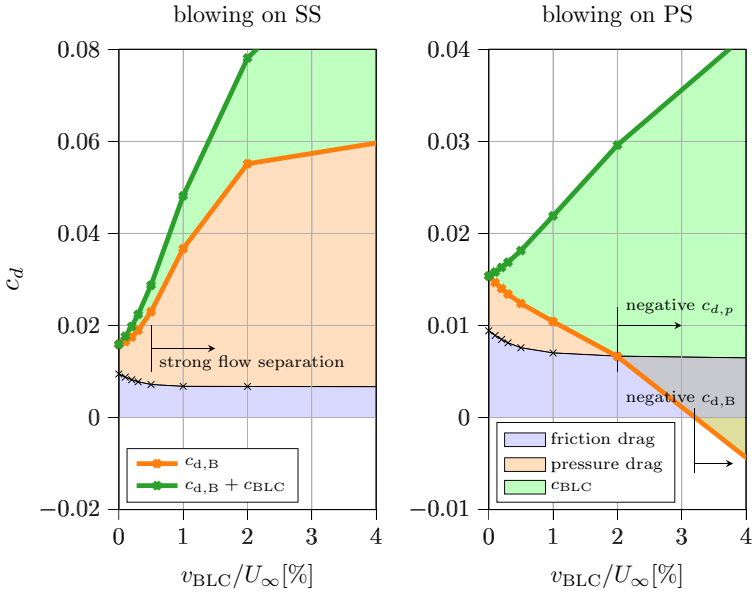

Fig. 4 Drag portion development for increasing intensity of uniform blowing on SS (left) and PS (right) for NACA 4412, $Re = 4 \cdot 10^5$, $\alpha = 5\circ$ based on incompressible RANS data

the momentum deficit in the wake which increases with increasing blowing rate since the added control mass flow rate has to be accelerated to U_∞.

As demonstrated, both the *body drag* as well as the *wake survey drag* carry a physical meaning. Whilst the information *body drag* conveys is trivial, since it describes the direct forces on the controlled body, the *wake survey drag* is at least as relevant, since it includes the crucial information of the unavoidable effort needed for the particular BLC scheme of uniform blowing. It has to be noted though, that the *wake survey drag* does not provide this information for all BLC control schemes. For laminar flow control via suction the *wake survey drag* underestimates the true effort and instead the *body drag* is a more reasonable quantity to look at in terms of BLC effort as pointed out by Beck et al. (2018). Therefore, we introduce the term *inclusive drag*, which we define as the drag quantity which includes the theoretical effort one has to put into enabling a certain boundary layer control scheme. We want to stress that this is not to be confused with the additional efforts related to particular implementation such as device power requirements, viscous losses of pipe flows, etc. In the case of uniform blowing the *inclusive drag* $c_{d,\text{inc.}}$ is represented by the *wake survey drag*. In the case of laminar flow control the *inclusive drag* is represented by the *body drag*.

The results discussed so far are also confirmed by the compressible data. Figure 5 shows the components of the drag coefficient for a control velocity of $v_{\text{BLC}} = 0.5\%U_\infty$ and an AoA of $\alpha = 0°$. In agreement with the previous results, blowing on the suction side leads to an increase in the *body drag* $c_{\text{d,B}}$ (in green) compared to the uncontrolled case. On the other hand, blowing on the pressure side results in a decrease of the body drag. The *wake survey drag* $c_{\text{d,W}}$ (in red) increases in both cases. In accordance with Eq. 8 the *wake survey drag* agrees with the sum of the *body drag* and the BLC penalty. As for the incompressible case, none of the two investigated cases lead to a reduction of the total drag coefficient, when taking into account the BLC penalty.

In Fig. 6 the effect of blowing velocity on the various drag components is shown. The left diagram shows the results for blowing on the suction side. The pressure drag (orange) increases with increasing blowing velocity, while the friction drag (blue) shows a small decrease. The strong adverse pressure gradient on the suction side in combination with blowing makes the flow prone to flow separation. This phenomenon can be observed from $v_{\text{BLC}} > 0.5\%U_\infty$. For a blowing velocity of $v_{\text{BLC}} > 1\%U_\infty$ the flow becomes unsteady and no convergence of the steady simulation can be reached, therefore only the data up until

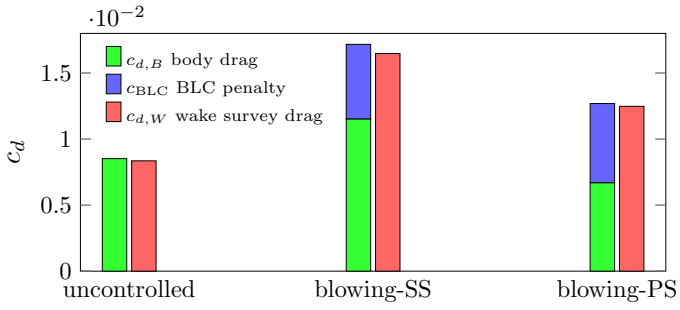

Fig. 5 Comparison of *wake survey* drag, *body drag* and *BLC penalty* based on compressible RANS data. NACA 4412, $Re = 5 \cdot 10^6$, $Ma = 0.4$, $v_{\text{BLC}} = 0.5\%U_\infty$, $\alpha = 0°$, $d_{\text{TE}}/c = 0.8$, $h/c = 1$

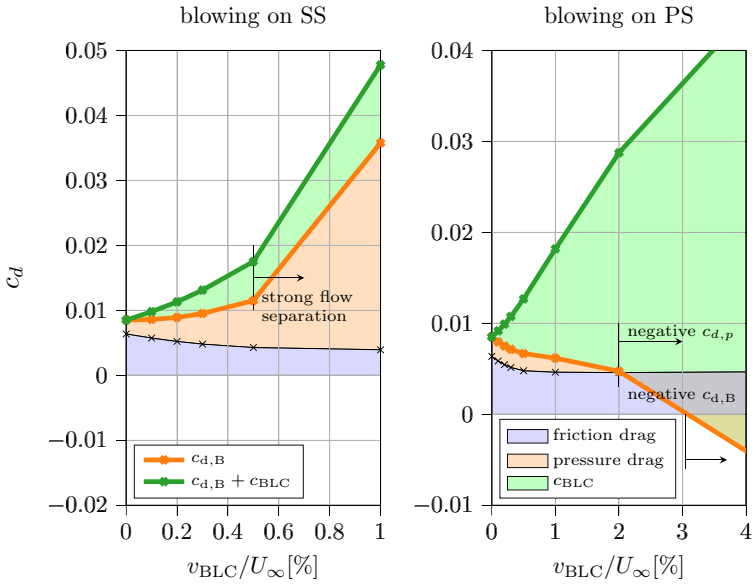

Fig. 6 Drag portion development for increasing intensity of uniform blowing on SS (left) and PS (right) for NACA 4412, $Re = 4 \cdot 10^5$, $\alpha = 0\circ$ based on compressible RANS data

$v_{BLC} = 1\%U_\infty$ are plotted in the figure. The BLC penalty increases with increasing blowing velocity and needs to be added to the *body drag*, as discussed before.

The figure on the right shows the results for blowing on the pressure side. A decrease in the friction drag can be observed, which reaches a constant level at $v_{BLC} = 1\%U_\infty$. As already seen in the incompressible case, the pressure drag decreases with increasing blowing velocity and becomes negative at $v_{BLC} > 2\%U_\infty$ in this particular case. A further increase in the blowing velocity leads to a change of sign in the *body drag* for $v_{BLC} > 3.05\%U_\infty$ due to the large negative drag contribution of the pressure drag.

3.2 Local Drag Assessment for Boundary Layer Flows

The previously discussed difference between *body drag* and *wake survey drag* and the relevance of the latter in determining the air intake effort do not only concern airfoil flows or external geometries but hold true also for flow control on a flat plate. This is the scenario in which micro blowing has been intensively investigated in the last decades (Kinney 1967; Simpson et al. 1969; Park and Choi 1999; Hwang 2004; Kametani and Fukagata 2011; Kametani et al. 2015; Stroh et al. 2016), mostly with a focus on the local skin friction drag reduction. In analogy to the discussion above, the wake of a finite size flat plate provides information about the corresponding inclusive drag. For the turbulent flow along the plate the momentum displacement boundary layer thickness δ_θ carries the same information as the wake, as discussed in the following.

The von Karman Eq. describes the spatial evolution of the boundary layer and its corresponding friction drag. In general form (Goldschmied 1951) with additional wall-normal transpiration v_{BLC} the dimensionless friction drag is usually scaled with the wall-parallel

free-stream velocity at the edge of the boundary layer at the same streamwise coordinate U_e:

$$\underbrace{2\frac{\tau_w}{\rho U_e^2}}_{c_{f,l}} + 2\frac{v_{\mathrm{BLC}}}{U_e} = 2\frac{d\delta_\theta}{dx} + 2\frac{2\delta_\theta + \delta^\star}{U_e}\frac{dU_e}{dx}. \tag{9}$$

The term $2v_{\mathrm{BLC}}/U_e$ can be simply moved to the right-hand side if one is interested in the local friction drag $c_{f,l}$, which is usually the case when studying canonical flows such as flat plate boundary layers. However, similar to the case of the 2D airfoil one can show that this term carries the information on the momentum penalty the system experiences for collecting BLC fluid from the free-stream. This motivates the interpretation of this term to be similar to the BLC penalty c_{BLC} described above. In order to have a more general view on the boundary layer of a flow around a body it is reasonable to rescale the Eq. with the velocity at infinity U_∞ which may differ from the velocity at edge of the boundary layer at the corresponding streamwise coordinate U_e in boundary layers with nonzero pressure gradients. Scaled with U_∞ the friction drag $c_{f,\infty}$ can be motivated alongside the local BLC-related penalty $c_{f,\mathrm{BLC}}$:

$$\underbrace{\underbrace{2\frac{\tau_w}{\rho U_\infty^2}}_{c_{f,\infty}} + \underbrace{2\frac{v_{\mathrm{BLC}}U_e}{U_\infty^2}}_{c_{f,\mathrm{BLC}}}}_{\text{inclusive drag } c_{f,\mathrm{inc}}} = \underbrace{2\frac{U_e^2}{U_\infty^2}\frac{d\delta_\theta}{d\bar{x}} + 2U_e\frac{2\delta_\theta + \delta^\star}{U_\infty^2}\frac{dU_e}{d\bar{x}}}_{\mathrm{RHS}}. \tag{10}$$

Similar to the wake survey the contribution of the Reynolds stresses is negligible, except at the edges of the controlled area (Stroh et al. 2016).

The Clauser parameter along the pressure side of the boundary layer on the NACA 4412 airfoil at $\alpha = 5\circ$ is plotted in Fig. 7b where $\beta \approx 0$ corresponds to ZPG conditions. The boundary layer assumptions are met if the value for β, i.e. $|\beta| \lessapprox 10$ and the streamwise slope $\partial\beta/\partial\bar{X}$ are sufficiently small. Otherwise, the assumption of the streamwise scales being large compared to the wall-normal scales is violated thus the boundary layer equations and also the von Karman equation loose their validity. As confirmed in Fig. 7a, on the PS of the uncontrolled airfoil the boundary layer assumptions are fulfilled, so the $c_{f,\infty}$ directly computed from the wall-shear stress corresponds to the derived RHS of von Karman Eq. 10. Application of blowing on the pressure side of the same airfoil results only in a minor modification of β as shown in Fig. 7b. Therefore, it is expected that the von Karman equation similarly holds when the blowing term $c_{f,\mathrm{BLC}}$ is included to estimate the *inclusive drag* coefficient $c_{f,\mathrm{inc}}$ along the plate. The corresponding results in Fig. 7a confirm this expectation.

In the large body of literature the control scheme of micro blowing has been considered in ZPG boundary layers along semi-infinite plates, i.e. flow scenarios without wake. The considerations above indicate that in these cases the momentum deficit of the boundary layer compensates not only the total force required to move the plate but also the supply of the control fluid (either by collecting it from the ambient or by carrying it). The aforementioned analysis for ZPG boundary layers can also be applied to the adverse pressure gradient boundary layer found on the suction side of the airfoil. In this case the values for β are progressively larger towards the aft of the airfoil which indicates an increasing adverse

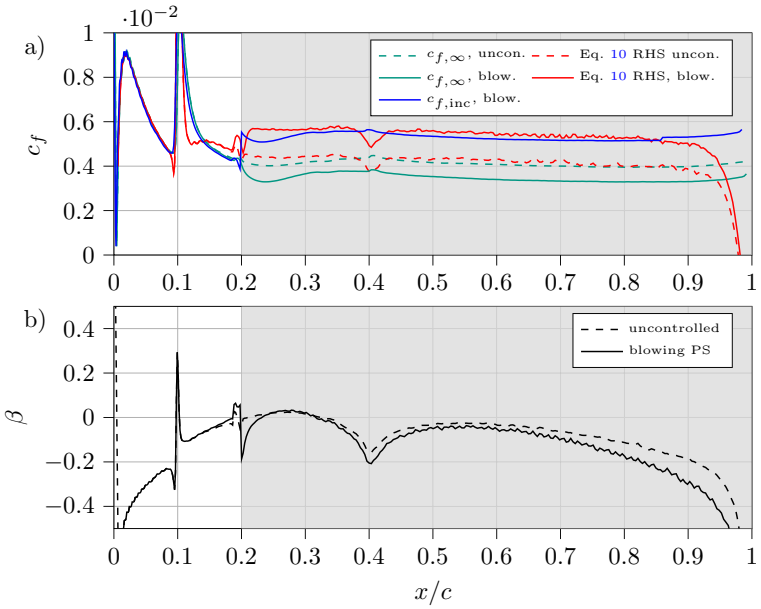

Fig. 7 Friction drag components (**a**) and Clauser parameter (**b**) on the pressure side of uncontrolled and controlled airfoil for NACA 4412, $Re = 4 \cdot 10^5$, $\alpha = 5\circ$ based on LES data. Grey-shaded area marks the location of control region

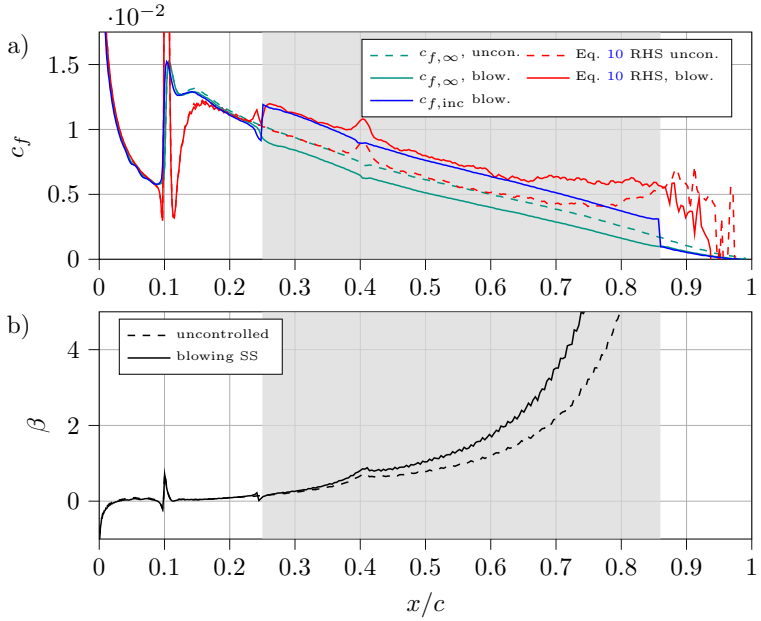

Fig. 8 Friction drag components (**a**) and Clauser parameter (**b**) on the suction side of uncontrolled and controlled airfoil for NACA 4412, $Re = 4 \cdot 10^5$, $\alpha = 5\circ$ based on LES data. Grey-shaded area marks the location of control region

pressure gradient. In this case the boundary layer approximation becomes less accurate which translates into less prominent agreement between $c_{f,\infty}$ and RHS of Eq. 10. Figure 8 shows the reasonable agreement of the two quantities for the uncontrolled case. It is also obvious that the difference between those quantities for the controlled case roughly corresponds to the BLC penalty c_{BLC}. This observation confirms that also for flat plate boundary layer investigations the concept of the *inclusive drag* has a physical correspondence to the boundary layer development derived through the von Karman integral equation. Since the *inclusive drag* is directly linked to the unavoidable costs of the BLC scheme of uniform blowing we stress that this important quantity has to be considered when judging control effectiveness also for flat plate boundary layer investigations, in which it has often been overlooked.

4 Conclusion

The present study exploits the global momentum balance to discuss a fundamental aspect of drag-reducing boundary layer control via wall-normal blowing, namely how to correctly quantify the drag force and its control-induced change.

The flow around an airfoil has been considered as application scenario of flow control. It is shown that the wall-normal blowing control modifies the relationship between the body drag $c_{\mathrm{d,B}}$, i.e. the drag force coefficient measured directly by integrating the stresses on the surface, and the wake survey drag $c_{\mathrm{d,W}}$, the drag force inferred indirectly via the momentum deficit in the wake of the airfoil. These two drag force coefficients are typically equal in an uncontrolled scenario or when a combination of blowing and suction results into zero net mass flux. With wall-normal blowing, however, a source of fluid mass is effectively applied at the airfoil surface if the air intake system providing the boundary layer control fluid is not explicitly considered. In this case, the flow control fluid expelled by the source initially lacks momentum in the main wind direction and is thus accelerated within the flow to wind speed while being deflected into the wake. Since the reaction force to such acceleration and deflection can only be carried by the body, the body drag $c_{\mathrm{d,B}}$ becomes smaller than the wake-survey drag $c_{\mathrm{d,W}}$ by an amount proportional to the blowing flow rate, which we name boundary layer control penalty c_{BLC}. We demonstrate that, in particular scenarios such as in absence of flow separation, the body drag can be even made negative and thus effectively turned to a thrust for sufficiently high blowing rates.

Both the body and wake-survey drag are legitimate measures of the drag force and carry a clear physical meaning, as discussed in the manuscript. The body drag $c_{\mathrm{d,B}}$ is the force effectively experienced by the body, as it could be measured by a drag balance, for instance. The wake-survey drag $c_{\mathrm{d,W}}$ plays a role akin to an inclusive (or net) drag, since it is the body drag augmented by the boundary layer control penalty c_{BLC}. This penalty is a reasonable estimate of the effort required to provide the boundary control fluid whenever this has not been already included by explicitly considering an air-intake system within the flow.

A simple thought experiment can clarify the distinction between body and wake survey-drag. Let a wing section with an airfoil geometry similar to the one considered in the present manuscript be placed into a closed-circuit wind tunnel with an open test section. Without wall-normal blowing control $c_{\mathrm{d,W}}$ and $c_{\mathrm{d,B}}$ would be equal. If wall-normal blowing is applied on the pressure side of the airfoil, thus not yielding flow separation, a drag balance attached to the wing will measure a value of body drag $c_{\mathrm{d,B}}$ smaller than the wake-survey

drag $c_{d,W}$ inferred from a pressure probe rake in the wake. Both measurements are completely correct: the body is experiencing a drag force proportional to $c_{d,B}$ while the wind tunnel fan needs to exert a force proportional to $c_{d,W}$ to maintain the same wind speed as in the uncontrolled case. In other words, the wind tunnel has to provide the additional force proportional to c_{BLC} required to accelerate the additionally injected flow control fluid and thus overcome the boundary layer control penalty.

We argue that the difference between body and wake-survey drag is responsible for the apparent contradicting results (discussed in Sect. 1) of laboratory and numerical experiments, in which respectively one of the two drag definitions is more widespread. The discussion of the difference and meaning of the body and wake-survey drag in presence of fluid sources, object of the present manuscript, may seem trivial at first to an expert aerodynamicist and has been discussed, albeit not directly in the context of flow control, in classic literature such as by [Schlichting and Gersten (2006), pag.311]. Nonetheless, recent works on the topic of turbulent drag reduction via wall-normal blowing (Ohashi et al. 2020; Kornilov 2021; Miura et al. 2022), including ours (Atzori et al. 2020; Fahland et al. 2021), overlooked this aspect or did not address it properly, thereby possibly overestimating the control performance by not considering the inclusive drag or pointing at an only apparent disagreement of the different drag measurements.

The relevance of the present study is not limited to flows around airfoils but also extends to other flows, such as flat-plate boundary layers, a widespread canonical scenario for studying flow control via wall-normal blowing (Kametani et al. 2016; Stroh et al. 2016; Mahfoze et al. 2019). Even though skin-friction is the only stress present on a section of an infinitely long plate, we have shown that also in such flows the inclusive drag — sum of the friction drag and the flow control penalty—is the relevant quantity for estimating realistically the net effect of the control and we advocate for its use in the future.

A last word must be spent regarding the overall performance of wall-normal blowing for drag reduction. In fact, when the inclusive drag is accounted for, none of the blowing cases addressed by Fahland et al. (2021) yields net drag reduction. However, in spite of the negative scenario for the potential of wall-normal blowing evoked by this result, there is still hope for this control strategy to show beneficial effects. In fact, wall-normal blowing could be an energy-efficient answer to the problem of the expulsion of flow collected elsewhere by suction flow control, whether it be for keeping the flow laminar or achieving high-lift configurations. Also, for the field of aircraft control, e.g. replacing classical ailerons, uniform blowing can be an interesting option as it has a positive coupling of lift and drag changes at the application position therefore preventing adverse yaw by role control.

A Estimation of BLC Fluid Supply Requirements

This example shall demonstrate the need to collect the fluid from freestream rather than bringing along a supply in case of a mobile application. For that purpose we assume more or less reasonable numbers of a passenger aircraft.

$$m_{BLC} = t \cdot \dot{m}_{BLC} = tcs\rho U_\infty \left(\frac{l_{BLC}}{c}\right)\left(\frac{v_{BLC}}{U_\infty}\right) = 280t \tag{11}$$

$$\text{with } t = 5h \quad \text{flight time} \tag{12}$$

$$c = 2\text{m} \quad \text{mean chord} \tag{13}$$

$$s = 35\text{m} \quad \text{span} \tag{14}$$

$$\rho = 0.4\text{kg/m}^3 \quad \text{density} \tag{15}$$

$$U_\infty = 800\text{km/h} \quad \text{speed} \tag{16}$$

$$\frac{l_{\text{BLC}}}{c} = 50\% \quad \text{BLC surface ratio} \tag{17}$$

$$\frac{v_{\text{BLC}}}{U_\infty} = 0.5\% \quad \text{blowing rate} \tag{18}$$

The BLC fluid accumulates to 280t of air which is at least two orders of magnitude above what such an aircraft could possibly bring along, not to mention the additional energy consumption or volume due to the added mass. This estimate shows that uniform blowing in mobile applications has to be provided by the same free-stream the body is subject to itself.

Author Contributions GF: design of the study, incompressible RANS data, manuscript draft. MA: LES data, its evaluation and discussion. AF: compressible RANS data, its evaluation and discussion. AS: discussion of boundary layer formulation, final text. BF: supervision and final text. DG: design of the study, supervision and final text.

Funding Open Access funding enabled and organized by Projekt DEAL. Partial financial support by the Elisabeth and Friedrich Boysen Foundation is greatly acknowledged.

Declarations

Conflict of interest The authors declare that they have no conflict of interest.

Ethical approval This work did not involve any active collection of human data.

References

Atzori, M., Vinuesa, R., Fahland, G., Stroh, A., Gatti, D., Frohnapfel, B., Schlatter, P.: Aerodynamic effects of uniform blowing and suction on a NACA4412 Airfoil. Flow Turbulence Combust **105**, 735–759 (2020). https://doi.org/10.1007/s10494-020-00135-z

Beck, N., Landa, T., Seitz, A., Boermans, L., Liu, Y., Radespiel, R.: Drag reduction by Laminar flow control. Energies **11**(1), 252 (2018). https://doi.org/10.3390/en11010252

Betz, A.: Ein Verfahren zur direkten Ermittlung des Profilwiderstandes. ZFM **16**, 42–44 (1925)

Bushnell, D.M.: Aircraft drag reduction-a review. Proc. Instit. Mech. Eng. Part G: J. Aerospace Eng. **217**(1), 1–18 (2003). https://doi.org/10.1243/095441003763031789

Dong, S., Karniadakis, G.E., Chryssostomidis, C.: A robust and accurate outflow boundary condition for incompressible flow simulations on severely-truncated unbounded domains. J. Comput. Phys. **261**, 83–105 (2014)

Economon, T., Palacios, F., Copeland, S., Lukaczyk, T., Alonso, J.: SU2: an open-source suite for multiphysics simulation and design. AIAA J. **54**(3), 828–846 (2016)

Eto, K., Kondo, Y., Fukagata, K., Tokugawa, N.: Assessment of friction drag reduction on a Clark-y airfoil by uniform blowing. AIAA J. **57**(7), 2774–2782 (2019). https://doi.org/10.2514/1.J057998

Fahland, G., Stroh, A., Frohnapfel, B., Atzori, M., Vinuesa, R., Schlatter, P., Gatti, D.: Investigation of blowing and suction for turbulent flow control on airfoils. AIAA J. **59**(11), 4422–4436 (2021). https://doi.org/10.2514/1.J060211

Fischer, P.F., Lottes, J.W., Kerkemeier, S.G.: NEK5000: Open source spectral element CFD solver. Available at: http://nek5000.mcs.anl.gov (2008)

Goldschmied, F.: Skin Friction of Incompressible Turbulent Boundary Layer Under Adverse Pressure Gradients. Technical report, National Advisory Committee for Aeronautics (1951)

Gregory, B.A., Walker, W.S., Devereux, A.N.: Wind-Tunnel Tests on the 30 per cent Symmetrical Griffith Aerofoil with Distributed Suction over the Nose. A.R.C. Technical Report 2647, Ministry of Supply, London (1953)

Hasanuzzaman, G., Merbold, S., Cuvier, C., Motuz, V., Foucaut, J.-M., Egbers, C.: Experimental investigation of turbulent boundary layers at high Reynolds number with uniform blowing, Part I: statistics. J. Turbulence **21**(3), 129–165 (2020). https://doi.org/10.1080/14685248.2020.1740239

Hirokawa, S., Ohashi, M., Eto, K., Fukagata, K., Tokugawa, N.: Turbulent friction drag reduction on Clark-Y airfoil by passive uniform blowing. AIAA J. (2020). https://doi.org/10.2514/1.J059627

Hosseini, S.M., Vinuesa, R., Schlatter, P., Hanifi, A., Henningson, D.S.: Direct numerical simulation of the flow around a wing section at moderate Reynolds number. Int. J. Heat Fluid Flow **61**, 117–128 (2016)

Hwang, D.: Review of research into the concept of the microblowing technique for turbulent skin friction reduction. Progress Aerospace Sci. **40**(8), 559–575 (2004). https://doi.org/10.1016/j.paerosci.2005.01.002

Jones, B.M.: The measurement of profile drag by the pitot traverse method. Technical Report 1688, Cambridge (1937)

Kametani, Y., Fukagata, K.: Direct numerical simulation of spatially developing turbulent boundary layers with uniform blowing or suction. J. Fluid Mech. **681**, 154–172 (2011). https://doi.org/10.1017/jfm.2011.219

Kametani, Y., Fukagata, K., Örlü, R., Schlatter, P.: Effect of uniform blowing/suction in a turbulent boundary layer at moderate Reynolds number. Int. J. Heat Fluid Flow **55**, 132–142 (2015). https://doi.org/10.1016/j.ijheatfluidflow.2015.05.019

Kametani, Y., Fukagata, K., Örlü, R., Schlatter, P.: Drag reduction in spatially developing turbulent boundary layers by spatially intermittent blowing at constant mass-flux. J. Turbulence **17**(10), 913–929 (2016). https://doi.org/10.1080/14685248.2016.1192285

Kinney, R.B.: Skin-friction drag of a constant-property turbulent boundary layer with uniform injection. AIAA J. **5**(4), 624–630 (1967). https://doi.org/10.2514/3.4039

Kornilov, V.: Combined blowing/suction flow control on low-speed airfoils. Flow Turbulence Combust **106**(1), 81–108 (2021). https://doi.org/10.1007/s10494-020-00157-7

Kornilov, V.I., Boiko, A.V.: Efficiency of air microblowing through microperforated wall for flat plate drag reduction. AIAA J. **50**(3), 724–732 (2012). https://doi.org/10.2514/1.J051426

Krishnan, K.S.G., Bertram, O., Seibel, O.: Review of hybrid laminar flow control systems. Progress Aerospace Sci. **93**, 24–52 (2017). https://doi.org/10.1016/j.paerosci.2017.05.005

Mahfoze, O.A., Moody, A., Wynn, A., Whalley, R.D., Laizet, S.: Reducing the skin-friction drag of a turbulent boundary-layer flow with low-amplitude wall-normal blowing within a Bayesian optimization framework. Phys. Rev. Fluids **4**, 094601 (2019). https://doi.org/10.1103/PhysRevFluids.4.094601

Menter, F.R., Kuntz, M., Langtry, R.: Ten years of industrial experience with the SST turbulence model. Heat. Mass Transf. **4**(1), 625-632 (2003)

Mickley, H.S.: Heat, mass, and momentum transfer for flow over a flat plate with blowing or suction. NACA, TN **3208**, 1–25 (1954)

Miura, S., Ohashi, M., Fukagata, K., Tokugawa, N.: Drag reduction by uniform blowing on the pressure surface of an airfoil. AIAA J. **60**(4), 2241–2250 (2022). https://doi.org/10.2514/1.J060831

Moffat, R.J., Kays, W.M.: The turbulent boundary layer on a porous plate: experimental heat transfer with uniform blowing and suction. Int. J. Heat Mass Transf. **11**(10), 1547–1566 (1968). https://doi.org/10.1016/0017-9310(68)90116-6

Norton, B.: STOL Progenitors: The Technology Path to a Large STOL Transport and the C-17A. American Institute of Aeronautics and Astronautics Inc, Reston, Va (2002)
Ohashi, M., Morita, Y., Hirokawa, S., Fukagata, K., Tokugawa, N.: Parametric study toward optimization of blowing and suction locations for improving lift-to-drag ratio on a Clark-Y airfoil. JFST **15**(2), 0008–0008 (2020). https://doi.org/10.1299/jfst.2020jfst0008
Park, J., Choi, H.: Effects of uniform blowing or suction from a spanwise slot on a turbulent boundary layer flow. Phys. Fluids. **11**(10), 3095–3105 (1999). https://doi.org/10.1063/1.870167
Patera, A.T.: A spectral element method for fluid dynamics: laminar flow in a channel expansion. J. Comput. Phys. **54**, 468–488 (1984)
Rumsey, C.L., Nishino, T.: Numerical study comparing RANS and LES approaches on a circulation control airfoil. Int. J. Heat Fluid Flow **32**(5), 847–864 (2011). https://doi.org/10.1016/j.ijheatfluidflow.2011.06.011
Russo, G.P.: Aerodynamic Measurements: from Physical Principles to Turnkey Instrumentation. Woodhead publishing in mechanical engineering. Woodhead Publishing, Cambridge ; Philadelphia, PA (2011). OCLC: ocn698329550
Schlatter, P., Stolz, S., Kleiser, L.: LES of transitional flows using the approximate deconvolution model. Int. J. Heat Fluid Flow **25**, 549–558 (2004)
Schlatter, P., Örlü, R.: Turbulent boundary layers at moderate Reynolds numbers: inflow length and tripping effects. J. Fluid Mech. **710**, 5–34 (2012)
Schlichting, H.: Grenzschicht-Theorie, 5, völlig neubearbeitete und erw, aufl Springer, Berlin (1964)
Schlichting, H., Gersten, K.: Boundary-layer Theory, 8th rev. and enl. ed edn. Springer, Berlin ; New York (2000)
Schlichting, H., Gersten, K.: Grenzschicht-Theorie Mit 22 Tabellen, 10., überarb. aufl edn. Springer, Berlin (2006). OCLC: 636610285
Schrauf, G.H., von Geyr, H.: Simplified Hybrid Laminar Flow Control for the A320 Fin - aerodynamic and system design, first results. In: AIAA Scitech 2020 Forum. American institute of aeronautics and astronautics, Orlando, FL (2020). https://doi.org/10.2514/6.2020-1536
Simpson, R.L., Moffat, R.J., Kays, W.M.: The turbulent boundary layer on a porous plate: experimental skin friction with variable injection and suction. Int. J. Heat Mass Transf. **12**(7), 771–789 (1969). https://doi.org/10.1016/0017-9310(69)90181-1
Spalart, P.R., McLean, J.D.: Drag reduction: enticing turbulence, and then an industry. Proc. R. Soc. A. **369**(1940), 1556–1569 (2011). https://doi.org/10.1098/rsta.2010.0369
Stroh, A., Hasegawa, Y., Schlatter, P., Frohnapfel, B.: Global effect of local skin friction drag reduction in spatially developing turbulent boundary layer. J. Fluid Mech. **805**, 303–321 (2016). https://doi.org/10.1017/jfm.2016.545
Sumitani, Y., Kasagi, N.: Direct numerical simulation of turbulent transport with uniform wall injection and suction. AIAA J. **33**(7), 1220–1228 (1995). https://doi.org/10.2514/3.12363
Townsend, A.A.: The Structure of Turbulent Shear Flow, 2d, ed Cambridge monographs on mechanics and applied mathematics. Cambridge University Press, Cambridge (1976)
Vinuesa, R., Negi, P.S., Atzori, M., Hanifi, A., Henningson, D.S., Schlatter, P.: Turbulent boundary layers around wing sections up to $Re_c = 1{,}000{,}000$. Int. J. Heat Fluid Flow **72**, 86–99 (2018). https://doi.org/10.1016/j.ijheatfluidflow.2018.04.017
von Glahn, U.H.: Use of the Coanda Effect for obtaining Jet Feflection and Lift with a single Flat-Plate Deflection Surface. Technical Note 4272, NACA, Cleveland, Ohio (1958)
Walsh, M.J.: Riblets for aircraft skin-friction reduction. Langley Symp Aerodyn. **1**, 557–571 (1986)
Weller, H., Tabor, G., Jasak, H., Fureby, C.: A tensorial approach to computational continuum mechanics using object-oriented techniques. Comput. Phys. **12**(6), 620–631 (1998)
Wilkinson, S.P., Anders, J.B., Lazos, B.S., Bushnell, D.M.: Turbulent drag reduction research at NASA Langley: progress and plans. Int. J. Heat Fluid Flow **9**(3), 266–277 (1988). https://doi.org/10.1016/0142-727X(88)90037-9